Custom made low-cost optoelectronic flex sensor and its parameterization

Luiza Amador Pozzobon[1] and Rodrigo da Silva Guerra[2]

***Abstract*— The use of flex sensors to evaluate the amount of bending of certain materials has many applications that range all the way from music creation to prosthetic devices. However, commercially available flex sensors are expensive and especially difficult to afford in developing countries, among which we cite as an example Brazil. Their high cost precludes their experimentation and usage in systems that demand a high number of sensors. With this thought in mind, this paper presents the design of a low-cost optoelectronic sensor, constructed with readily available simple materials, such as a coil spring, a LED and an LDR sensor. Parameterization tests were performed to evaluate its functioning limits. It can be concluded that the reflective nature of the spring assists with the propagation of the light projected inside it, ensuring that the illumination is not interrupted early in the bending motion. The optimal sensor length is of 3 cm since it presented the most stable and consistent results.**

I. INTRODUCTION

Flex sensors are used in a wide range of applications, from joint position estimation to earthquake detection or musical creation [1]–[3]. Commercially available sensors, that generally make use of capacitive technologies or conductive ink, can be quite expensive. In developing countries, like Brazil, each flex sensor is available at a cost that ranges from U$18.91 to U$67.11 in most common electronic stores, quoted in Brazilian Reais in August 2019. The elevated cost of electronic devices such as these harms the scientific prosperity of countries that fit the profile. It acts as a hurdle to the development of projects, especially ones that demand the use of multiple sensors, such as sensory gloves [4] and prosthetic devices.

In this paper, we present a possible solution to the described problem: the manufacture of a low-cost optoelectronic flex sensor and its parameterization. In Section II, the related work is presented. Section III introduces the materials and methods used in the construction and parameterization of our flex sensor. In Section IV and V are the results and their discussion, respectively.

II. RELATED WORK

A. *Resistive flex sensors*

The most commonly available flex sensors are the ones with conductive ink, which return resistance values. Its functioning scheme is presented in Fig. 1. Generally, those sensors allow a bidirectional reading, bending in a single axis, backward and forwards. They are available in many sizes, from 1 to 4.5 inches (or 2.54cm to 11.43cm).

B. *Parameterization*

One of the general parameterizations available by manufacturers is the *'R versus θ'* graph. It is an assessment of the sensor's operation, a relation between its returned resistance value to each bending degree [6]. A curve that depicts a usual flex sensor can be seen in Fig. 2. Other examples of parameterization tests found in the literature are the (1) sensitivity, (2) repeatability, (3) hysteresis and (4) relaxation tests, as done by [5].

The sensitivity evaluation consisted of rotating the sensor from 0° to the maximum range permitted by the test structure. The resistance change from zero to the maximum degree is plotted and fitted within a linear function, which is defined as the sensitivity measurement.

The repeatability evaluation consists of rotating the sensor within a certain range, with 1 Hz of frequency, for both clockwise and counterclockwise rotations, for a total of 20 cycles. The sensor's value is normalized to its maximum and minimum recorded values, and then the variance for each of the bending angles is calculated. In this experiment, the smaller variance indicates better repeatability.

The hysteresis test corresponds to the normalized area between clockwise and counterclockwise slopes, in order to evaluate the "time-based dependence of a system's output on present and past inputs" [5]. In this experiment, the smaller the hysteresis, the less variation in readings to each of the bending degrees, resulting in reliable readings disregarding which direction the system is moving.

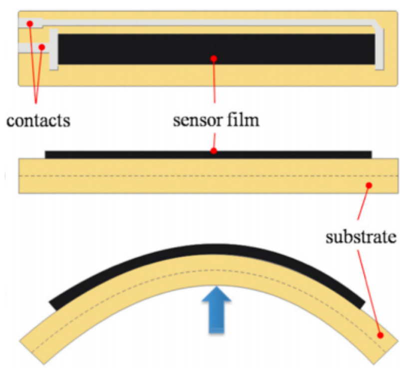

Fig. 1: Commercial ink-based flex sensor scheme.

[1]Luiza Amador Pozzobon is an undergraduate student of Control and Automation Engineering at Federal University of Santa Maria, Santa Maria - RS, Brazil. luiza.pozzobon@gmail.com

[2]Rodrigo da Silva Guerra is with the Department of Electrical Engineering at Federal University of Santa Maria, Santa Maria - RS, Brazil. At the time of development of this project, he was a visiting scholar at National Taiwan Normal University. rodrigo.guerra@ieee.org

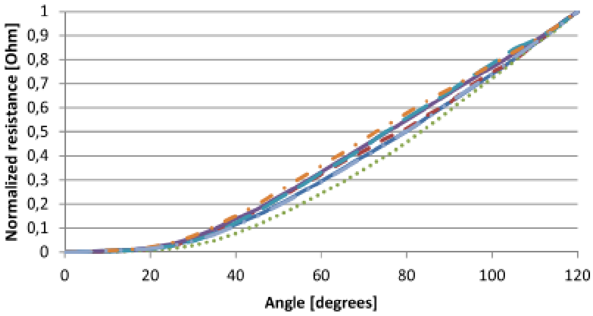

Fig. 2: *'R versus θ'* graph for a commercially available flex sensor as presented by [6].

The last experiment presented, the relaxation test, investigates the amount of time the signal takes to reach its stabilization. The time of signal settling corresponds to "the moment in when the sensor signal does not change within 5 mV for five seconds" [5].

III. MATERIALS AND METHODS

As mentioned previously, we opted to design our own low-cost optoelectronic flex sensor, due to the high cost of commercially available ones. Our sensor is designed under principles of optoelectronics [7], such as the one presented in [8], applied to a prosthetic hand, which served as an inspiration to this project.

In our flex sensor, there is an extension coil spring of 6mm of external diameter with two electronic components at its terminations: an LDR sensor and an LED, as observed in Fig. 3 scheme. With this construction arrangement, the more the spring is bent, the less light from the LED reaches the LDR sensor. In this setting, the reflection generated by the reflective surface of the metal spring ensures that at least some light intensity reaches the LDR. The power circuit for the LDR, powered at 5 V, is a simple voltage divider to ensure the expected numerical accuracy, and the returned value is higher the more light it detects, acting as a "light sensor".

The resistor value of the voltage divider, 10 kΩ, was set in view of the minimum and maximum resistance values that the LDR can achieve, according to its datasheet[1], for minimum and maximum brightness, respectively. The high brightness LEDs used require a 3.3 V power supply, and we make use of 68 Ω resistors to limit their voltages.

[1]LDR Light Sensor Datasheet: https://www.sunrom.com/get/443700

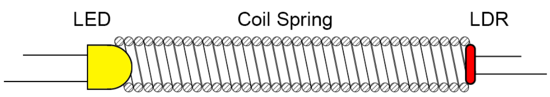

Fig. 3: Scheme of the flex sensor design that we propose in this work.

A. Parameterization

To validate the sensor's usage, we performed similar evaluations as the ones presented in Section II: the repeatability, the hysteresis, and the stability tests. Although usually the results are presented in terms of resistance, we chose to present it in volts, with a minimum value of 0 V and a maximum of 5 V. Additionally, we made a few changes to the testing details, such as the way we present the results. The parameterizations were performed in a manner that each sensor was coupled with one end attached to the side of a ROBOTIS Dynamixel MX-28 servo actuator. The other end had partial movement in order for the rotations and bending angles variations to be applied.

The parameterization was performed in light of our desired application for the sensor: a prosthetic hand and curvature estimation for its fingers. According to [3], the maximum bending angle of a finger joint is less than 120°, therefore our testings were performed within this range (from 0° to 120°).

The repeatability and hysteresis evaluation tests made use of the same data, which was captured in the following format:

1) Set servomotor to initial state: this is considered its 180°position, in which the sensor is relaxed, as in Fig. 4 (a);
2) Rotate the motor 10° at a time until it reaches the minimum position of 60°, in which the sensor is flexed, as in Fig. 4 (b);
3) At each angle position, the returned valued from the sensor is captured;
4) Do the same, but counterclockwise, from 60° to 180°;
5) The procedure from 1 to 4 was repeated ten times (ten batches).

Finally, the system's stability evaluation differed from the ones presented previously in terms of sensitivity range. We put the sensor to move in the clockwise direction, from 180° to 60°, from 10° at a time, like before. At each of the set angles, we recorded the amount of time it took for the sensor's value to stabilize in the range of 0.2 V (minus or plus 0.1 V) for five seconds.

(a) Actuator at 180°. Sensor extended.

(b) Actuator at 60°. Sensor flexed.

Fig. 4: Flex sensor coupled to servomotor in order to perform the evaluation tests.

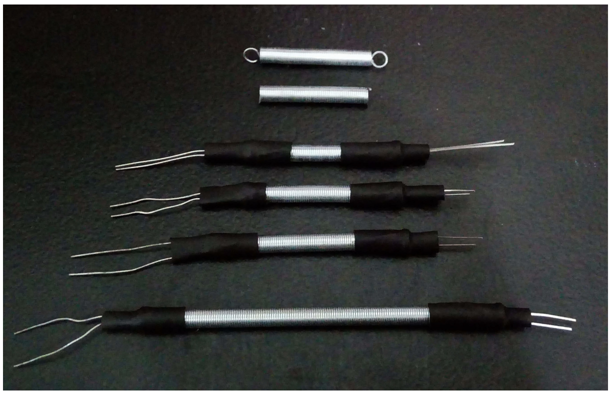

Fig. 5: From bottom to top: 7 cm sensor, 3.5 cm sensor, 3 cm sensor and the 3 cm springs before the coupling of electronics.

IV. RESULTS

In order to investigate the performance of different length sensors, as [3], we evaluated three pairs of different spring lengths, shown in Fig. 5: two sensors with 3 cm, two with 3.5 cm and two with 7 cm springs. In this section, sensors 0 and 1 correspond to the 3 cm spring length, sensors 2 and 3 to 3.5 cm, and sensors 4 and 5 to 7 cm. Note that all tests were conducted in the same environment and under the same conditions.

A. Repeatability Test

The repeatability test aims to investigate the degree of repeatability of the sensor, i.e. whether the readings for the same bending angles are consistent at different periods of time. In Fig. 6, we can observe the comparison of standard deviation (SD.) expressed in terms of percentage regarding each bending angle for commercial flex sensors and the ones presented at this paper.

In Fig. 6 (a), are the findings as displayed in [3], which were obtained with a ten times iteration of their repeatability test. They performed this experiment for four types of commercial flex sensors, three of them are manufactured by Flexpoint: the first is coated with polyamide, the second with polyester, the third is uncoated (with no lamination on top of it), the fourth is manufactured by SpectralSymbol and referenced as SS. In Fig. 6 (b) are the values obtained for our custom flex sensors 0 and 1 with the methods described previously. We chose to demonstrate the results for this pair of sensors due to their performance in the next sections, which are far superior than the others (sensors 2 to 5).

It's possible to note that our custom flex sensors are competitive with commercially available ones. It presents consistent results until the bending of 110° analyzing specifically sensor 0, since sensor 1 was slightly inferior. The higher SD. variation from 110° to 120°, when the sensor is almost fully flexed, indicates the probable beginning of light interruption from the LED to the LDR due to the intense bending. It's important to emphasize that until a bending of

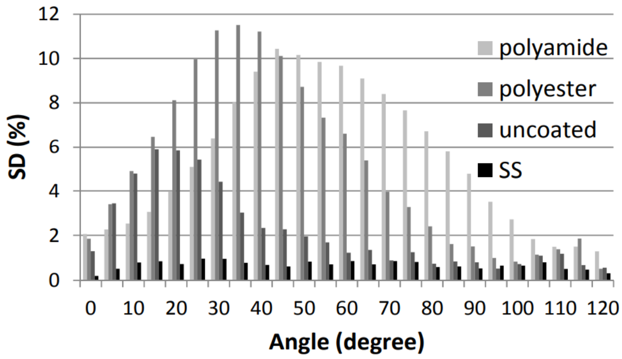

(a) Results obtained from commercially available sensors, as presented in [3]

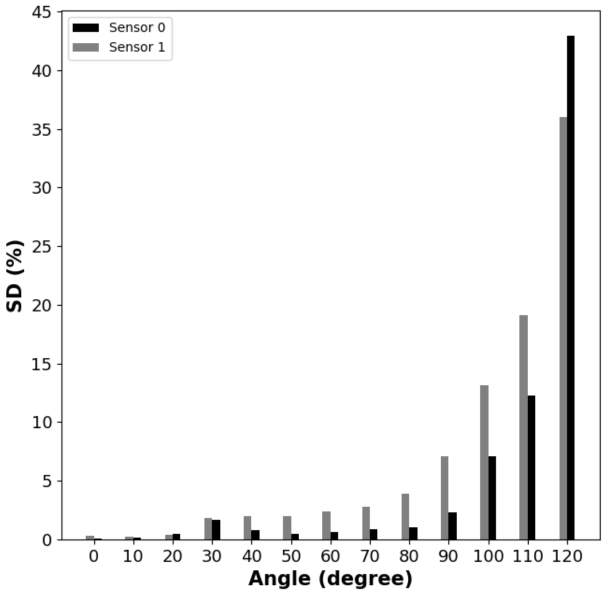

(b) Results obtained for the flex sensors 0 and 1 presented in this paper.

Fig. 6: SD. (%) versus bending degree for commercial and our custom-made flex sensor.

80°, sensor 0 shows a SD. percentage comparable to the best commercial flex sensors presented, the SS and the uncoated.

B. Hysteresis Test

Fig. 7 presents the normalized hysteresis results for the 3 cm, 3.5 cm and 7 cm spring sensors respectively. The average value of the ten readings of each angle is taken. Then, these values are averaged again for the ten test repetitions, both clockwise and counterclockwise. This last averaged value represents a point on the hysteresis graph.

C. The influence of light

The materials used for the manufacture of these sensors lead to another question: what is the influence of ambient light on their behavior? With the flexing of the sensor, the extension spring of its body opens, allowing external light to interfere in the reading of the LDR sensor. Thus, two

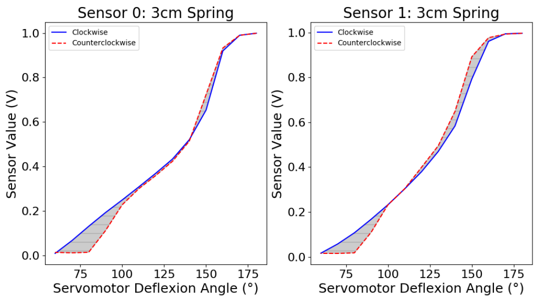

(a) Sensors 0 and 1: 3 cm spring

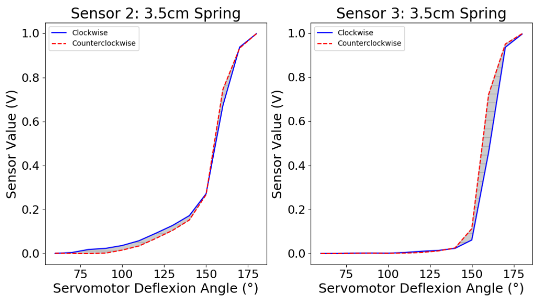

(b) Sensors 2 and 3: 3.5 cm spring

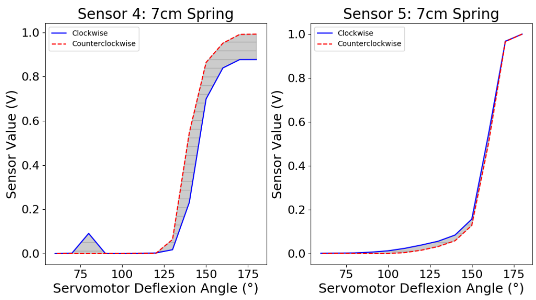

(c) Sensors 4 and 5: 7 cm spring

Fig. 7: Hysteresis graphs for the pairs of 3 cm, 3.5 cm and 7 cm sensors. Solid blue curve represents the clockwise movement, while the dashed red curve is the counterclockwise.

other repeatability and hysteresis tests were performed: one with a diffuse flashlight, and another with a concentrated flashlight, of approximately 650 and 11000 lux, respectively. The flashlights were aimed at the LDR sensor, always rigidly coupled to the test system, at a distance of about 15 cm. The Fig. 8 shows light sources pointed towards the system.

It is noteworthy that the first repetition and hysteresis tests were performed in the ambient light of approximately 50 lux. Only sensors 0 and 1 were subjected to these testings, since they seemed to perform better at the hysteresis evaluation, as will be discussed in the next section.

Fig. 9 shows the comparison of ambient light readings versus 650 lux diffuse flashlight readings for both 3 cm sensors. In Fig. 10 are the comparisons between the testings in ambient light versus those the concentrated light of 11000 lux. The values presented are calculated in the same way as the hysteresis of the previous section.

In addition, Table I and Table II present both absolute and quadratic errors of the counterclockwise and clockwise curve pairs compared, as well as Pearson's correlation coefficient for diffuse and concentrated illumination versus the ambient illumination, respectively. If the result of this coefficient is closer to the unitary value, the greater the positive correlation between the curves, if it is closer to the negative unitary value, the greater the negative correlation between them and, if zero, the curves have no correlation. Finally, Table III shows the mean standard deviation values, corresponding to the repeatability test, for the two new light conditions of sensors 0 and 1.

D. *Stability Test*

Table IV shows the results of settling time obtained for the pairs of 3.5 cm and 7 cm sensors. In Table V the values obtained for the different light conditions from the last subsection, for sensors 0 and 1, are also presented. It is noteworthy that this experiment was performed right after the previous ones so that the coupling of each sensor is identical in all tests to which it was submitted.

V. DISCUSSION

A. *Hysteresis*

According to the results, both 7 cm and 3.5 cm sensors have similar behaviors: a high variance (indicated by the steep slope of the curve) for a given reading range, and a low variance for the remaining readings. For 7 cm sensors, the high variance can be observed from the test angles of 130° to 180°, while for 3.5 cm sensors this behavior is observed from 150° to 180°.

In addition, the testing instability of these sensor lengths is observed. For both lengths, one of the tested elements has significantly lower quality than the other. Sensors 3 and 4, of 3.5 cm and 7 cm, respectively, for example, have nearly stagnant readings from 60° to 120° when compared to their pairs, sensors 2 and 5, which still do not show a good, linear, variation rate.

A good amount of the problems mentioned are minimized by further reducing the length of the spring. Both 3 cm sensors tested have higher reading linearity and substantially more stable behavior: there are no major behavioral discrepancies between the two elements, in contrast to what was found with the 3.5 cm and 7 cm pairs.

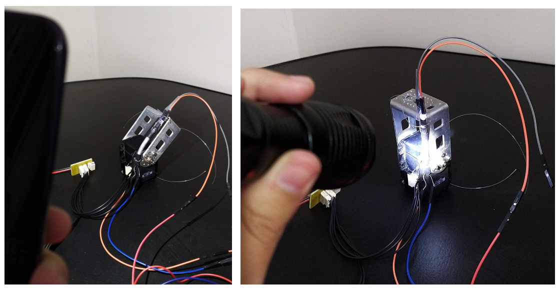

(a) Diffuse light of about 650 lux.
(b) Concentrated light of 11000 lux.

Fig. 8: The distance of light sources to the testing system.

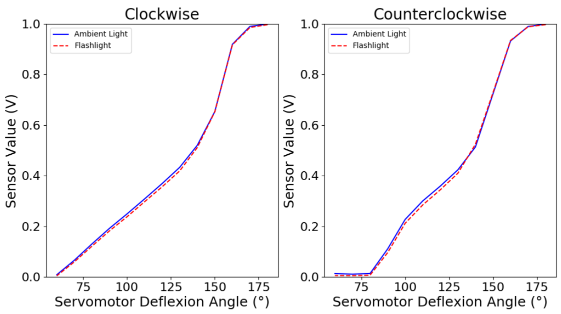

(a) Sensor 0 at 650 lux.

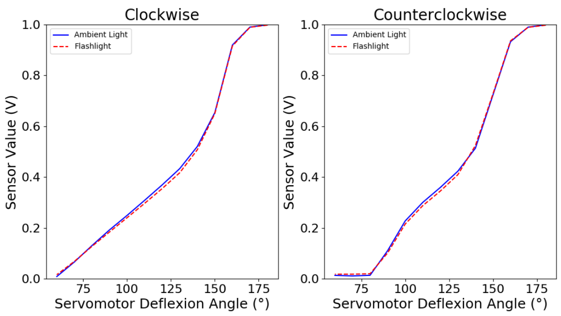

(b) Sensor 1 at 650 lux.

Fig. 9: Comparison of clock and counterclockwise curves for sensors 0 and 1 with 650 lux diffuse light source.

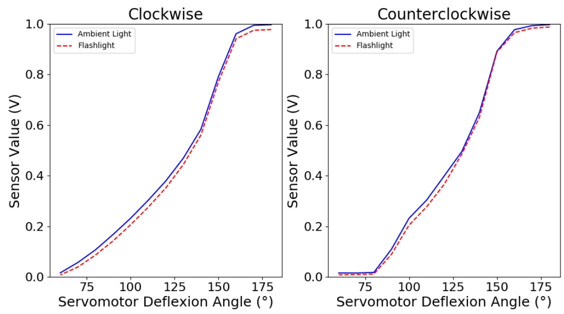

(a) Sensor 0 at 11000 lux.

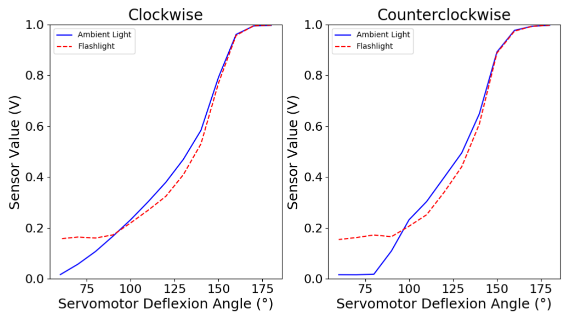

(b) Sensor 1 at 11000 lux.

Fig. 10: Comparison of clock and counterclockwise curves for sensors 0 and 1 with 11000 lux light source.

Both the larger hysteresis area, between 60° and 100°, and curve's plateau from 170° to 180° readings, are probably due to the difficulty of their coupling to the test system. Because they were smaller in size, their fixation to the servomotor was quite complex, so that there was a looseness in the movement from 170° to 180° (although the actuator moved, the sensor only rotated in position without being bent).

B. *The influence of light*

When studying the comparison graphs of the diffuse light and the ambient light tests, it is observed that there is interference from the outer light to which the sensor is subjected. However, quite reduced for the lux variation in this case.

On the other hand, when we look at the comparative graphs for ambient light versus 11000 lux light, there are discrepant results. Sensor 1 has a greater distinction in readings, especially between the values of 60° and 90°, where it is in intense flexion. In addition, it presents a greater variation between readings for the other angles when compared to the intensity of 650 lux. Sensor 0, on the other hand, does not show large variations in the results obtained in relation to diffuse light.

TABLE I: Absolute error, quadratic error, in Volts, and Pearson correlation from the sensors 0 and 1 curves with ambient light (50 lux) versus diffuse light (650 lux).

		Sensor 0	Sensor 1
Clockwise	**Abs. Error**	0.09678	0.2804
	Quad. Error	0.0009	0.0064
	Pearson Corr.	0.9999	0.9999
Counter Clockwise	**Abs. Error**	0.1152	0.1898
	Quad. Error	0.0014	0.0039
	Pearson Corr.	0.9998	0.9997

TABLE II: Absolute error, quadratic error, in Volts, and Pearson correlation from the sensors 0 and 1 curves with ambient light (50 lux) versus concentrated light (11000 lux).

		Sensor 0	Sensor 1
Clockwise	**Abs. Error**	0.0947	0.5484
	Quad. Error	0.0010	0.0454
	Person Corr.	0.9998	0.9875
Counter Clockwise	**Abs. Error**	0.1001	0.7334
	Quad Error	0.0010	0.0790
	Pearson Corr.	0.9997	0.9834

Thus, it is found that, yes, the light to which the sensors are subjected can significantly impact the reading values. However, there is a possibility to prevent such a problem from occurring, since sensor 0 does not present it. It is believed that the variability of readings between the sensors 0 and 1 for the light differences is due to the disparity in their coupling to the testing system. Probably, sensor 0 was coupled to the servomotor so that the spring was not so intensely opened in the regions near the LDR sensor, avoiding that the external light influenced it considerably, at least for the source light angle adopted for these tests.

Finally, it is noted that the different light conditions did

TABLE III: Mean standard deviation (SD.), corresponding to the repeatability test, of the batch of ten tests for each of the sensors, in volts, of sensors 0 and 1, under diffuse (650 lux) and concentrated (11000 lux) light conditions.

	Diffuse Light		**Concentrated Light**	
	Sensor 0	**Sensor 1**	**Sensor 0**	**Sensor 1**
Mean SD.	0.0024	0.0056	0.0060	0.0243

TABLE IV: Settling time, in seconds, of sensors 2 to 5 under ambient light conditions.

	Sensor 2	**Sensor 3**	**Sensor 4**	**Sensor 5**
180°	0.0214	0.0219	0.0224	0.0819
170°	0.0217	0.0216	0.0221	0.0217
160°	0.0219	0.0218	1.3279	0.4240
150°	0.1222	0.0214	0.0222	0.2228
140°	0.0216	1.3266	0.0215	8.8594
130°	0.0218	3.3341	1.8276	3.7374
120°	0.0215	0.9241	2.1269	0.0215
110°	0.0215	11.0659	0.0191	0.4227
100°	0.0213	0.8226	0.0193	0.0209
90°	0.0209	11.4627	0.0192	0.0199
80°	0.0213	0.0191	0.0192	2.4287
70°	0.0208	5.6408	0.0193	0.0197
60°	0.0202	0.0192	0.0189	1.5251
Mean	0.0291	2.6694	0.4220	1.3697
Length Mean	1.34925		0.89585	

TABLE V: Settling time, in seconds, of sensors 0 and 1 under each of the luminosity conditions.

	Ambient		**Diffuse**		**Concentrated**	
	0	**1**	**0**	**1**	**0**	**1**
180°	0.0803	0.0220	0.0742	0.0818	0.0815	0.0743
170°	0.0224	0.0221	0.0219	0.0218	0.0223	0.0224
160°	0.0219	0.0221	0.0219	0.0219	0.0221	0.0223
150°	0.0219	0.0222	0.0220	0.0224	0.0218	0.0224
140°	0.0224	0.0222	0.0223	1.9303	0.0222	0.0223
130°	0.9260	0.0224	0.0224	0.0224	3.7390	0.0221
120°	6.7508	0.0218	0.0223	0.0213	0.8252	0.0225
110°	1.8297	0.0213	0.0222	0.0222	15.0868	0.0223
100°	0.0218	0.0221	0.0223	0.0218	1.7289	0.0217
90°	0.0219	0.0213	0.0219	0.0220	0.0221	0.0219
80°	0.0209	0.0211	2.5316	0.0217	0.1218	0.0217
70°	2.2310	0.0215	0.5240	0.0215	0.1221	0.0221
60°	0.0217	0.0215	8.1563	0.0215	5.8462	0.0220
Mean	0.9225	0.0218	0.8835	0.1733	2.1278	0.0262
Lum. Mean	0.4722		0.5284		1.0770	

not generate significant errors, at least numerically, between the compared curves. Moreover, when considering the values of sensor 1 in the concentrated light test, it is observed that the decrease in the Pearson correlation is of approximately 0.016 compared to those obtained for diffuse light. This also indicates that even the difference between the curves presented in the comparative graph was not sufficient to unrelate them.

C. Stability

Although there are some points where the sensors took a larger amount of time to reach stability for 5 seconds, in most of them it is achieved almost instantly, with timings of less than 0.03 seconds. It is noted that with the increase of the external lighting intensity, the time of accommodation of the sensor values also tends to increase. This is verified by observing the increasing averages of settling times for each of the light conditions in Table V.

The overall cost to manufacture one sensor is about U$2.03, with prices from the LED, LDR, and spring quoted in Brazilian Reais in August 2019, being of U$0.34 for the first and of U$0.89 for the last two items.

VI. CONCLUSION

This paper presented the design and parameterization of a custom optoelectronic flex sensor. In contrast to commercially available ones, that make use of conductive ink, our sensor relies on a light receptor (an LDR) sensor, and a light emitter (an LED). These components were attached to a coil spring, through which the light circulates. It can be concluded that the reflective nature of the metal assists the propagation of light projected inside it, in order to ensure that the illumination is not interrupted early in the bending motion. However, the repeatability test results indicates that the light could be suffering from slight interruption, which could demand a small reduction in length from the 3 cm sensor analyzed in that section. After the parameterization testings, the optimal sensor length was found to be the one made of a 3 cm coil spring, since it presented the most stable and consistent results. It was also extremely competitive with respect to the best evaluated commercial flex sensors when observing the standard deviation presented as a percentage. We identify shortcomings in this project, such as the lack of a fatigue test of the materials used and the absence of modulation to undermine the influence of light into the values returned by the sensor. Such frailties should be further examined in future work.

REFERENCES

[1] Waseem Afzal, Shamas Iqbal, Zanib Tahira, and Mehtab Ejaz Qureshi. Gesture control robotic arm using flex sensor. *Applied and Computational Mathematics*, 6(4):171–176, 2017.

[2] Sreejan Alapati and Shivraj Yeole. A review on applications of flex sensors. *International Journal of Emerging Technology and Advanced Engineering*, 7:97–100, 07 2017.

[3] Giovanni Saggio, Antonio Pallotti, Laura Sbernini, Vito Errico, and Franco Di Paolo. Feasibility of commercial resistive flex sensors for hand tracking applications. *Sensors & Transducers*, 201(6):17, 2016.

[4] Satjakarn Vutinuntakasame, V-ris Jaijongrak, and Surapa Thiemjarus. An assistive body sensor network glove for speech-and hearing-impaired disabilities. In *2011 International Conference on Body Sensor Networks*, pages 7–12. IEEE, 2011.

[5] Dong Hyun Kim, Sang Wook Lee, and Hyung-Soon Park. Sensor evaluation for soft robotic hand rehabilitation devices. In *2016 6th IEEE International Conference on Biomedical Robotics and Biomechatronics (BioRob)*, pages 1220–1223. IEEE, 2016.

[6] Giovanni Saggio, Francesco Riillo, Laura Sbernini, and Lucia Rita Quitadamo. Resistive flex sensors: a survey. *Smart Materials and Structures*, 25(1):013001, 2015.

[7] Thomas G Zimmerman. Optical flex sensor, September 17 1985. US Patent 4,542,291.

[8] Huichan Zhao, Kevin OBrien, Shuo Li, and Robert F Shepherd. Optoelectronically innervated soft prosthetic hand via stretchable optical waveguides. *Science Robotics*, 1(1):eaai7529, 2016.